TISSUE ENGINEERING: Part A
Volume 29, Numbers 5 and 6, 2023

DOI: 10.1089/ten.tea.2022.0177

termis
Tissue Engineering
& Regenerative Medicine
International Society

ORIGINAL ARTICLE

Fast Degradable Calcium Phosphate Cement for Maxillofacial Bone Regeneration

Bart van Oirschot, DDS, PhD,[1] Antonios G. Mikos, PhD,[2] Qian Liu, PhD,[3–5]
Jeroen J.J.P. van den Beucken, PhD,[1,6] and John A. Jansen, DDS, PhD[1,6]

The aim of this preclinical study was to test the applicability of calcium phosphate cement (CPC)-poly(lactic-co-glycolic acid) (PLGA)-carboxymethylcellulose (CMC) as a bone substitute material for guided bone regeneration (GBR) procedures in a clinically relevant mandibular defect model in minipigs. In the study, a predicate device (i.e., BioOss®) was included for comparison. Critical-sized circular mandibular bone defects were created and filled with either CPC-PLGA-CMC without coverage with a GBR membrane or BioOss covered with a GBR membrane and left to heal for 4 and 12 weeks to obtain temporal insight in material degradation and bone formation. Bone formation increased significantly for both CPC-PLGA-CMC and BioOss with increasing implantation time. Further, no significant differences were found for bone formation at either 4 or 12 weeks between CPC-PLGA-CMC and BioOss. Finally, bone substitute material degradation increased significantly for both CPC-PLGA-CMC and BioOss from 4 to 12 weeks of implantation, showing the highest degradation for CPC-PLGA-CMC (~85%) compared to BioOss (~12%). In conclusion, this minipig study showed that CPC-PLGA-CMC can be used as a bone-grafting material and stimulates bone regeneration to a comparable extent as with BioOss particles. Importantly, CPC-PLGA-CMC degrades faster compared to BioOss, is easier to apply into a bone defect, and does not need the use of an additional GBR membrane. Consequently, the data support the further investigation of CPC-PLGA-CMC in human clinical trials.

Keywords: calcium phosphate, cement, bone defect, minipig model, bone regeneration

Impact Statement

Guided bone regeneration (GBR) is a frequently used dental surgical technique to regenerate the alveolar ridge to allow stable implant installation. However, stabilization of the GBR membrane and avoidance of bone graft movement remain a challenge. Consequently, there is need for the development of alternative materials to be used in GBR procedures that are easier to apply and induce predictable bone regeneration. In this minipig study, we focused on the applicability of calcium phosphate cement-poly(lactic-co-glycolic acid)-carboxymethylcellulose as an alternative bone substitute material for GBR procedures without the need of an additional GBR membrane.

[1]Department of Dentistry—Regenerative Biomaterials, Radboud University Medical Center, Nijmegen, The Netherlands.
[2]Department of Bioengineering (MS142), Rice University, Houston, Texas, USA.
[3]Department of Stomatology, Tongji Medical College, Union Hospital, Huazhong University of Science and Technology, Wuhan, China.
[4]School of Stomatology, Tongji Medical College, Huazhong University of Science and Technology, Wuhan, China.
[5]Hubei Province Key Laboratory of Oral and Maxillofacial Development and Regeneration, Wuhan, China.
[6]Radboud Institute for Molecular Life Sciences, Nijmegen, The Netherlands.

Introduction

Dental implants act as a replacement for single or multiple lost teeth and are used to support a crown, bridge, or removable prosthesis. The number of people receiving dental implants is still increasing yearly, which is due to their high success rate in restoring oral function and facial appearance of a patient.[1] The surgical procedure for implant placement involves the drilling of a hole in the alveolar bone for the stable insertion of a dental implant. However, frequently, the height or width of the alveolar bone is insufficient to achieve a solid base for the implant due to, for example, trauma during tooth extraction, infections, periodontal pathology, as well as the naturally occurring resorption of the alveolar bone after tooth extraction.[2,3]

Various studies reported that about 25% of the alveolar bone volume disappears within 1 year after tooth extraction, which can increase to 4–60% within 3 years after extraction.[4–7] The lack of sufficient bone volume for the solid fixation of a dental implant also has an unfavorable effect on the early- and long-term prognosis of dental implants.[8]

Guided bone regeneration (GBR) is a dental surgical technique to reestablish the contour and regenerate the alveolar ridge at sites with insufficient bone quantity to allow stable implant installation.[9] The GBR procedure entails a barrier membrane in combination with a bone grafting procedure. The bone graft material as installed functions as a filler of the bone defect site, provides a scaffold for the deposition of new bone from the surrounding bone, and has to support the osteogenic differentiation of mesenchymal cells. The barrier membrane that is used to cover the bone graft material has to maintain the created space and excludes the ingrowth of epithelium and connective tissue into the defect.[10]

A successful GBR-procedure depends on several key factors, including patient selection and wound conditions at the defect site as well as the used type of membrane and graft material.[11] Considering patient selection, smoking, diabetes, and previous administration of bisphosphonates are risk factors that can interfere with wound healing. The criteria for the barrier membrane are biocompatibility, space creation and maintenance, exclusion of undesirable cell types, integration with surrounding tissues, and clinical handling.[12] Since their introduction in the 80s, a wide variety of membranes have been developed, which can roughly be divided in two groups, that is, resorbable and nonresorbable membranes, and are all associated with advantages and disadvantages.[8,12,13] Resorbable as well as nonresorbable membranes play an essential role in the GBR treatment. Nonresorbable membranes have well-described space-maintaining and biocompatible characteristics.[14–16]

However, nonresorbable membranes need an additional surgical intervention for removal of the membrane. Resorbable, mainly collagen-based, membranes on the contrary can overcome the need for additional surgery. The downside of these membranes, however, is their limited mechanical strength and fast degradation that can cause a collapse of the bone defect.[15] Also, difficult handling properties have been reported when using these types of membranes.[16] Both types of membranes are associated with the risk of exposure of the membrane, which can lead to infection and subsequent premature removal of the membrane.[15]

As bone-grafting material, the most used materials are autogenous bone, xenografts (mostly deproteinized bovine bone mineral), and synthetic bone substitutes (calcium phosphates [CaPs]). Currently, there is no clear evidence that any specific bone graft substitute is superior in terms of bone regeneration.[11] Further, it has to be emphasized that to ensure successful GBR, primary wound closure, sufficient blood supply, and stability of the applied materials have to be achieved.[17] A tension-free primary wound closure can be challenging to achieve and frequently requires the use of specific surgical techniques.[18] Stabilization of the GBR membrane and avoidance of bone graft movement are accomplished by placing titanium pins through the barrier membrane to fix it on the buccal and lingual/palatal bone.

However, if a resorbable membrane is used, membrane resorption can be too rapid and result in loss of bone graft stability as well as cell-occlusive effects.[14] In addition, the titanium pins have to be removed, which requires a second surgical procedure. Thus, there is still need for the development of alternative materials to be used in the GBR procedure, which are easier to apply and induce predictable bone regeneration.

Such an alternative treatment modality is the use of calcium phosphate cement (CPC).[19,20] CPCs are self-setting materials, which are composed of CaP powder and a liquid. After mixing these components, a paste is formed, which can be shaped according to the defect dimensions after installation and subsequently hardens *in situ* through a dissolution and reprecipitation process into a micro- or nanoporous structure.[21] Consequently, an optimal contact will be formed between the tissue and CPC. Besides, CPCs are osteoconductive due to their CaP nature. Also, the additional application of a membrane is not necessary, as the set CPC will completely fill the defect and seal it from the ingrowth of unwanted cells.

Depending on the end product as formed during the setting reaction, two different types of CPC can be discerned, that is, brushite or apatitic CPC.[22] The main difference between these two types of CPC is their solubility and mechanical strength. Brushite CPCs are more soluble and resorb very fast *in vivo*.[23] In addition, they have very short setting time, which makes it necessary to add lots of liquid during the mixing process.[24] This results in a highly porous CPC with a low mechanical strength, which limits the clinical application.[24] In contrast, apatitic CPCs possess more appropriate clinical handling properties and a high mechanical strength, which makes them more suitable for clinical application[25]

However, a disadvantage of apatitic CPCs is their dissolution and resorption rate, as the end product of the setting reaction is calcium deficient hydroxyapatite (HA), which is poorly soluble and resorption is completely dependent on active degradation by osteoclasts, giant cells, or macrophages.[26] Ideally for clinical application, the biodegradation rate of CPC is almost similar to the rate of new bone formation at the defect site to allow for gradual regeneration of the bone defect. An approach to increase the degradation of apatitic CPC is by creating porosity into the cement. Pores with a size of 1–100 μm will significantly increase the surface area for the migration and proliferation of osteoclasts as well as osteoclasts and macrophages into the cement, which will result in an enhanced degradation.[27]

One of the most widely used methods to create porosity in CPC is by the combination of the bioceramic powder phase with degradable polymeric microparticles, such as poly(lactic-co-glycolic acid) (PLGA). After mixing the powder phase with liquid and setting of the created paste, the polymeric microparticles will be homogeneously dispersed throughout the CPC and will subsequently degrade hydrolytically resulting in porosity. Also, if PLGA is used for microparticle manufacturing, the degradation product due to hydrolytic degradation of the PLGA microparticles will result in a decrease of the pH into the cement, which will have a multiplier effect on cement degradation.[28]

Other important factors for the clinical application of CPCs are injectability and cohesion of the material after injection in a wet environment. Optimization of injectability and cohesion can be achieved by the addition of the non-toxic, hydrophilic polymer carboxymethylcellulose (CMC) into the CPC formulation. CMC has binding properties to CaP particles, which improves the cohesion of the material.[21] In a recent long-term implantation study of the CPC-PLGA-CMC in critical size rabbit condyle defects, as performed in our laboratory, >90% material degradation with concomitant bone regeneration was demonstrated over a 26-week period.[21] Interestingly, these results were obtained without the placement of a GBR membrane to prevent soft tissue ingrowth, which confirms that CPC-PLGA-CMC sufficiently hinders soft tissue penetration into the bone defect.

In view of the above-mentioned, we hypothesized that CPC-PLGA-CMC would be suitable as a moldable bone substitute with appropriate handling properties for cranio-maxillofacial bone regenerative treatment without the need for the use of an additional GBR membrane. To test this hypothesis, we used a clinically relevant minipig model,[29] histology and histomorphometry as endpoint analyses as well as a predicate device (i.e., BioOss, the no. 1 dental bone substitute material and standard of care[30,31]) for comparison. Critical-sized circular mandibular bone defects were created and filled with either CPC-PLGA-CMC without coverage with a GBR membrane or BioOss covered with a GBR membrane and left to heal for 4 and 12 weeks to obtain temporal insight in material degradation and bone formation.

Materials and Methods

Implantation material

CPC-PLGA was composed of 60 wt.% milled, pure alpha tricalciumphosphate (α-TCP) powder with a mean particle size of ~4.0 μm (CAM Bioceramics B.V., Leiden, The Netherlands) and 40 wt.% PLGA powder with a mean particle size of ~60 μm and lactic:glycolic acid ratio 50:50; molecular weight of 17 kDa; and acid-terminated (Corbion Purac® B.V., Gorinchem, the Netherlands). Carboxymethylcellulose (CMC; Blanose 9H4XF-PH; Barentz International B.V., Hoofddorp, The Netherlands) was added to the CPC-PLGA for optimization of the cohesive properties of the CPC to inhibit outwash of the cement paste in highly vascularized or bleeding bone defects. The used CMC had a particle size of ≤106 μm (Ashland Industries Europe GmbH, Alizay, France) and was proportionally added at 1.5 wt.%. A 4 w/v% sodium dihydrogen phosphate dihydrate aqueous solution ($NaH_2PO_4.H_2O$) was used as liquid to create the cement paste.

Before implantation, all powder components of the CPC-PLGA-CMC were sterilized by gamma irradiation at a minimum dose of 25 kGy (Synergy Health Ede B.V., Ede, The Netherlands). The NaH_2PO_4 solution was filter sterilized (pore size by 0.22 μm). The CPC-PLGA-CMC powder was mixed using a spatula with the NaH_2PO_4 solution at a liquid-to-powder ratio of 0.5 mL g^{-1} to obtain a homogeneous moldable paste.

BioOss S demineralized bone mineral granules (Geistlich Pharma AG, Wolhusen, Switzerland) with a particle size of 0.25–1 mm was used as predicate device. A BioGuide GBR membrane (Geistlich Pharma, Wolhusen, Switzerland) was used to cover bone defects filled with the BioOss S granules. The membrane was cut to size during surgery and fixed to the bone with mini-titan fixation pins (Botis Dental, Berlin, Germany).

CPC-PLGA-CMC characterization

X-ray diffraction (XRD) analysis was performed ($n = 3$) to determine the crystal phase of the CPC-PLGA-CMC. Set CPC-PLGA-CMC was incubated for 7 days in phosphate buffered saline (PBS) at 37°C to allow full phase transformation. After 7 days, samples were freeze-dried, ground to powder, and analyzed by powder XRD (X'Pert[3] Powder; PANalytical Almelo, the Netherlands). XRD spectra were registered at 2Θ from 10° to 60°, a step size of 0.02° and a counting time of 1 s. XRD spectra of α-TCP and HA powders were used as control.

The initial and final setting time of the CPC-PLGA-CMC ($n = 3$) was assessed using Gillmore needles (ASTM C266). Therefore, the CPC-PLGA-CMC was mixed with the NaH_2PO_4 solution and the resulting paste was molded into a bronze mold provided with holes of 6 mm diameter and 12 mm height, which was subsequently placed in a water bath of 37°C. The Gillmore needles were lowered onto the cement paste and the initial and final setting time were recorded if penetration of the needles into the cement paste did not occur anymore. To assess the effect of CMC on the setting properties, initial and final setting was also determined for CPC-PLGA without the addition of CMC.

Cohesion of CPC is the ability of the paste to set in an aqueous environment without disintegration. CPC-PLGA-CMC as well as CPC-PLGA were loaded into a 5 mL syringe ($n = 3$). Subsequently, the paste was injected into PBS solution of 37°C after 90 s of creating the paste. Upon immersion, the cohesion was qualitatively assessed according to degree of particulate cloud formation and fragmentation.

Animal species

Sixteen adult female Göttingen minipigs (Ellegaard, Delmose, Denmark) were used to assess bone defect regeneration at two healing periods, that is, 4 and 12 weeks. The number of animals was based on statistical power analysis. The primary outcome parameter in the study design was bone formation. Based on earlier studies, bone formation was estimated to be around 20–30% with a standard deviation (SD) of 15%.[32] Sample size was calculated based on a two-way analysis of variance (ANOVA) with an alpha of 0.05, SD of 15%, and an effect size of 30%. The required group size for each healing time and

experimental material was estimated to be eight defects, which corroborated other minipig study data for bone regeneration.[33]

Surgical procedure

All surgical procedures were performed according to ARRIVE Guidelines at the Radboudumc Animal Research Facility after the Dutch Central Committee on Animal Research and the local Ethics Committee of the Radboud University on Animal Research approved the study under project license AVD1030020197984 and protocol 2019-0006 respectively.

For an extensive description of the surgical procedure and the used materials reference can be made to a recent publication of van Oirschot et al.[34] In brief, after induction of general anesthesia, the anterior region of the left or right side of the mandible was shaved and cleaned with chlorhexidine (5 mg/mL in 70% ethanol). Subsequently, mesial from the first molar, an extraoral subangular incision was made bilaterally to expose the lateral portion of the anterior region of the mandibular body. The incision was made through the fascia and muscle and the bone was exposed by blunt dissection. Then, full thickness standardized circular defects, comprising removal of the buccal mandibular cortex, were made using a trephine dental drill with an outer diameter of 8 mm. The buccal cortex had a thickness of about 4 mm.

During drilling, sterile saline was used to prevent heating of the drill and to protect the surrounding bony structures. The defects were filled with CPC-PLGA-CMC or BioOss S granules. Materials were equally distributed over defects by means of randomization. The BioOss S-filled defects were covered with a rectangular shaped membrane, which was fixed at the corners with mini-titan pins. After implantation of the bone graft materials, the soft tissues were closed in multiple layers using resorbable Vicryl 3-0 sutures Ethicon, Norderstedt, Germany). For closure of the skin, a continuous intracutaneous suture technique was used. Immediate postoperative pain was controlled by a buprenorphine patch (20 μg/hour; Butrans, Mundipharma Pharmaceuticals B.V., Belgium) and meloxycam (5 mg/mL; Novem, Boehringer, Germany) was given per os 24 h after surgery. The animals were checked daily for any possible infections.

Animals were divided into two groups ($n=8$) and defects were allowed to heal for 4 and 12 weeks. At the end of the designated healing period, animals were euthanized following the required sample size ($n=8$) for each healing time and experimental material. The mandibles were harvested, excess soft tissue was removed and with a circular saw the mandibular body was further reduced in length by removing the distal and mesial parts that contained teeth to ~ 4 cm in length. After removal of the bone marrow, the bone segments were placed in 4% phosphate-buffered formaldehyde solution (pH 7.2).

Histological preparation

After fixation in 4% formaldehyde for 14 days, the specimens were dehydrated in a graded series of ethanol concentrations (70–100%), after which they were embedded in polymethylmethacrylate (pMMA). After polymerization, thin sections of about 10 μm in thickness were prepared in a transverse plane perpendicular on the longitudinal direction of the mandible using an inner diamond blade microtome (Leica Microsystems SP 1600, Nussloch, Germany). The first section of each specimen was aimed at the center of the defect and additional sections were made by continuing mesial or distal from the first section. All sections were stained with methylene blue and basic fuchsine. At least, three sections of the center area of the defect were used for histological and histomorphometric analysis.

Histological and histomorphometric analysis

The stained sections of the various defects and implantation times were assessed by light microscopy (Leica Microsystems AG, Wetzlar, Germany). Histomorphometric analysis of the sections was performed using ImageJ computer-based image analysis software (ImageJ 2.0.0-rc-43/1.52n; Java 1.6.0_24). From digitalized images of the sections, a rectangular shaped region of interest (ROI) of 6×2 mm was positioned over the defect, leaving 1 mm free of the defect border. If the diameter of the defect in the sections had a different size, the ROI was adapted accordingly. Within the ROI, the contours of newly formed bone, BioOss, and soft tissue were drawn manually (Wacom Cintiq 16; Wacom Co., Ltd., Kazo, Japan).

After drawing, the contours were filled, and the images were converted to binary images. With the measurement function of ImageJ, the total area of newly formed bone as well as the amount of CPC-PLGA-CMC and BioOss in the defect were subsequently quantified and expressed as percentage of the total ROI area.

Statistics

All data are presented as mean values and SD. Differences between groups and time points were assessed by unpaired Student's *t*-test using SPSS Statistical Program (Version 27; IBM). The level of statistical significance was set at $p < 0.05$ (two-tailed).

Results

CPC-PLGA-CMC characterization

XRD analysis revealed that the CPC-PLGA-CMC had fully transformed into HA after 7 days of incubation in PBS. The characteristic diffraction peaks of α-TCP had disappeared and the major reflection peaks of HA were

Table 1. Initial and Final Setting Times (Min) of Calcium Phosphate Cement (CPC)-Poly (Lactic-Co-Glycolic Acid) (PLGA) and CPC-PLGA-Carboxymethylcellulose Cements

CPC	*Initial setting time (min)*	*Final setting time (min*
CPC- PLGA	5.0 ± 0.5	18.3 ± 0.3
CPC-PLGA-CMC	5.7 ± 0.3	18.7 ± 0.2

$n=3$ for all specimens.

$p > 0.05$. No significant differences between CPC-PLGA and CPC-PLGA-CMC.

CMC, carboxymethylcellulose; CPC, calcium phosphate cement; PLGA, poly(lactic-co-glycolic acid).

FIG. 1. CPC-PLGA-CMC composite paste injected into a saline solution immediately after preparation (within 3 min). CMC, carboxymethylcellulose; CPC, calcium phosphate cement; PLGA, poly(lactic-co-glycolic acid).

revealed at $2\Theta = 25.9°$, 31.7°, 32.2°, 39.8°, 46.7°, 49.6°, and 53.3°. Addition of CMC did not affect phase transformation.

As depicted in Table 1, initial setting time of the CPC-PLGA-CMC was found to be 5.7 ± 0.3 min, while final setting was 18.7 ± 0.2 min. The initial setting of the CPC-PLGA without CMC was 5.0 ± 0.5 min with a final setting time 18.3 ± 0.3 min. Statistical analysis indicated that the initial and final setting time of the CPC-PLGA-CMC were comparable with CPC-PLGA ($p > 0.05$).

The cohesion test demonstrated that the addition of CMC strongly improved the cohesive properties and injectability of the CPC-PLGA (Fig. 1).

Animal model

During surgery, it appeared that the cement paste could easily be applied and molded according the defect shape. Cement setting occurred within a few minutes according the predetermined setting time.

Further, the minipigs showed an uneventful postoperative healing. No clinical complications or inflammatory response was observed. Wound healing progressed without any problem and all animals remained healthy during the entire experimental period. At the end of the various implantation times, all specimens could be retrieved.

Histological evaluation

BioOss S granules—4 weeks: Light microscopical examination of the sections showed that the bone defect could easily be recognized, as well as the installed BioOss particles. Remnants of the GBR membrane were seen in seven of the specimens and were recognized as a thin grayish layer with a granular appearance (Fig. 2A). Particles filled the bone defect completely and extended always into the bone marrow cavity. No tight contact existed between the BioOss particles and the bone defect borders. In all sections, woven callus formation had occurred at the periosteal and endosteal side of the bone defect borders. In seven of the specimens, the woven callus formation was limited, while in one specimen, extensive callus formation was seen, which covered completely the buccal side of the bone defect (Fig. 2B).

For this specimen, extensive bone formation was found between the BioOss particles; however, ingrowth was limited to the upper part of the bone defect and characterized by a bony connection between the particles at the buccal side of the defect as well as a tight contact between the particles and the surrounding bone (Fig. 2B). In five of the specimens, no bone formation was found in between the BioOss particles. In these specimens, fibrous tissue was present between the particles (Fig. 2C). There was no evidence of an inflammatory response, and the number of inflammatory cells was very limited. In two of the specimens, early signs of bone formation were observed between the BioOss particles, as illustrated by the bridging of bone trabeculae bridging between the particles (Fig. 2D).

CPC-PLGA-CMC—4 weeks: Light microscopy showed that all defects were completely filled with cement, which did extend into the bone marrow cavity and was in very tight

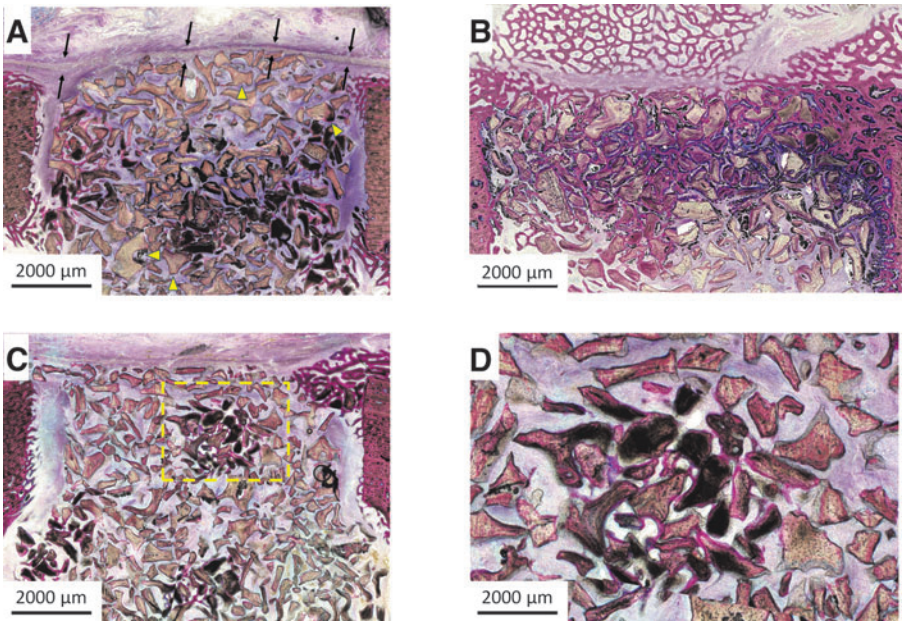

FIG. 2. Histological cross sections of minipig mandibular bone defects filled with BioOss® particles after 4 weeks of healing following embedding in MMA, sectioning using an inner circular diamond saw, and staining with methylene blue/basic fuchsin (original magnification ×400). **(A)** BioOss particles-filled defect after 4 weeks of implantation with remnants of GBR membrane (*black arrows*) and large installed BioOss particles (*yellow triangles*). **(B)** Extensive callus formation covering completely the buccal side of the bone defect. **(C)** Early signs of bone formation between BioOss particles. **(D)** Higher magnification of bone trabeculae bridging between the particles. GBR, guided bone regeneration; MMA, methylmethacrylate.

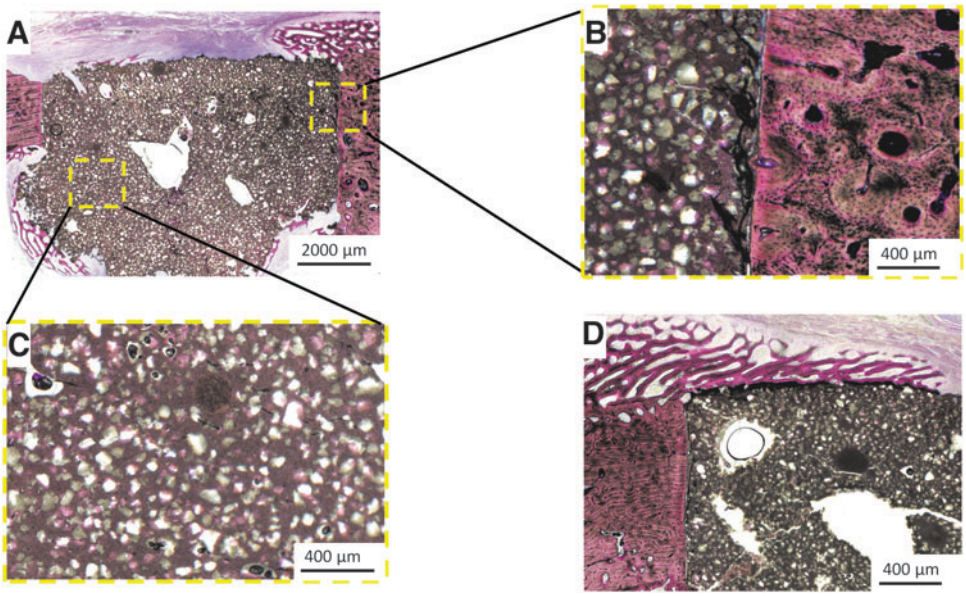

FIG. 3. Histological cross sections of CPC-PLGA-CMC bone defects after 4 weeks of healing (original magnification ×400). **(A)** Complete filling of the defect, extending into the bone marrow cavity. **(B)** CPC-PLGA-CMC in full contact with original defect margins. **(C)** Higher magnification of CPC-PLGA-CMC-filled defect with a pinkish material suggesting osteoid-like tissue. **(D)** Bone formation on the cement surface at the periosteal and endosteal side of the defect.

contact with the bone defect borders. Micropores and some macropores were observed into the cement. Gross degradation of the cement was not present and no inflammatory cells were seen. At the defect borders, no bone formation had occurred. At the periosteal and endosteal side of the bone defect, always woven bone formation was seen (Fig. 3A), which was growing over the cement and was in close contact with the cement surface (Fig. 3B). Higher magnification revealed that a major part of the cement micropores were filled with a pinkish material suggesting the presence of osteoid-like tissue (Fig. 3C). Bone was not only seen at the periosteal side, but also at the endosteal side bone formation occurred on the cement surface (Fig. 3D).

BioOss S granules—12 weeks: Histological analysis indicated that the bone defects as well as the defect borders could still be recognized (Fig. 4A). The BioOss particles were still present in the bone defect, but in all defects, bone had grown in between the particles and all defects were completely closed with newly formed bone. The gap between the particles and bone defect was always found to be bridged by immature bone, characterized by a woven morphology.

Bone formation was mainly limited to the BioOss particles in the bone defect and did not extend into the particles as present in the bone marrow cavity. The bone formed in between the particles was always in tight contact with the particle surface. The present bone voids were filled with bone marrow-like tissue. No osteoclasts or inflammatory cells were found. In all sections, a bone response was seen at the periosteal and endosteal side of the bone defect. In some sections, still some remnants of the GBR membrane seemed to be present (Fig. 4B).

CPC-PLGA-CMC—12 weeks: Light microscopical examination showed that the CPC-PLGA-CMC had almost completely degraded. Only, cement remnants were visible at the endosteal side of the bone defect or where the cement was extending into the bone marrow cavity (Fig. 5A). Larger remnants of CPC-PLGA-CMC were surrounded by bone, which was in close contact with the cement surface (Fig. 5B). The space, as created by cement degradation, was occupied by bone with a trabecular appearance (Fig. 5B). If the cement had extended into the bone marrow cavity, bone had grown in between the cement and was penetrating in the bone marrow cavity as well.

Bone formation occurred from the periosteal and endosteal side of the bone defect as well as the defect borders (Fig. 5C). At the periosteal side, the bone was observed to be denser compared with the center or the endosteal side, starting to resemble on the native cortical bone at the sides of the bone defect (Fig. 5D). In the bone voids, bone marrow-like tissue and cement remnants were seen, but no inflammatory cells or osteoclasts were observed.

Histomorphometric analysis

Material degradation. Histomorphometric results concerning material degradation are presented in Table 2. The

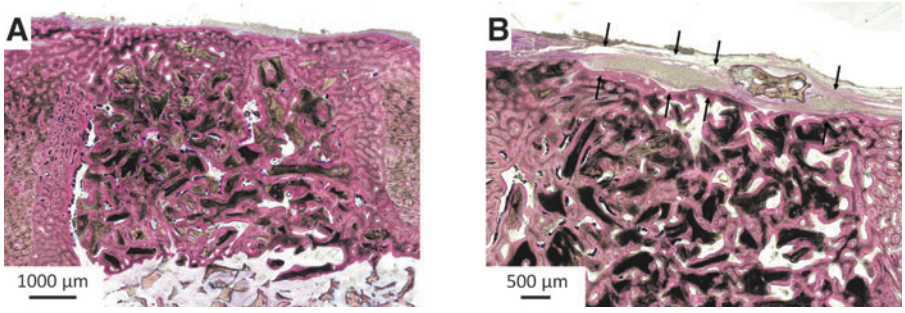

FIG. 4. Histological cross sections of BioOss-filled defects after 12 weeks of healing. **(A)** Bone ingrowth in between the particles and complete coverage of the defect with newly formed bone. **(B)** Remnants of the GBR membrane as depicted by the *black arrows*.

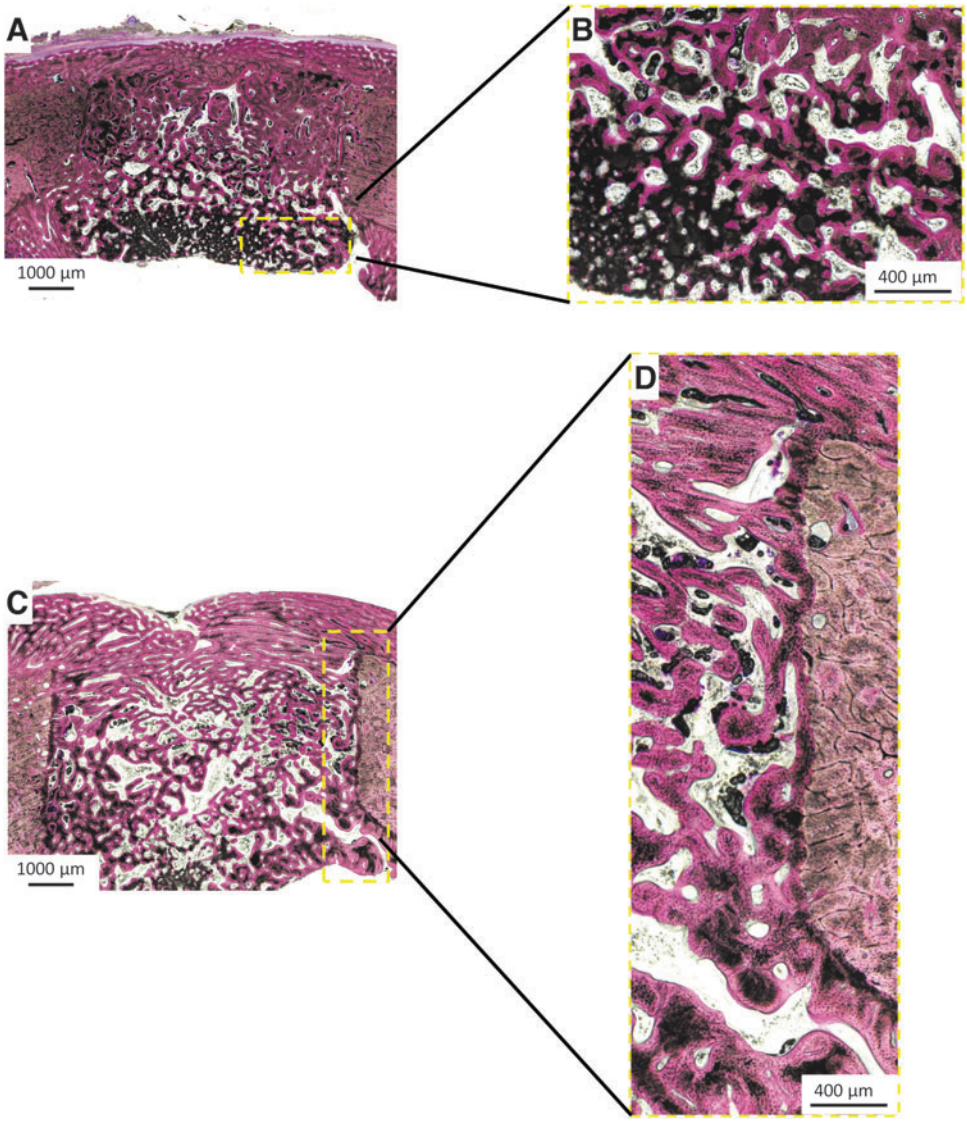

FIG. 5. Histological cross sections of CPC-PLGA-CMC-filled defects after 12 weeks of healing. **(A)** Almost complete degradation of the CPC-PLGA-CMC cement with cement remnants at the endosteal side of the defect (*yellow box*). **(B)** Higher magnification of cement degradation and trabecular bone formation in between the cement. **(C)** Bone formation from the endosteal, periosteal side, as well as from the original margins of the bone defect. **(D)** Higher magnification of cement remnants as well as dense bone at the periosteal side of the defect, resembling native cortical bone.

amount of material as left in the bone defects decreased significantly for both BioOss ($p<0.05$)—and CPC-PLGA-CMC ($p<0.001$) from 4 to 12 weeks of implantation, but CPC-PLGA-CMC showed significantly lower material remnant values at 12 weeks compared to BioOss ($p<0.001$). The CPC-PLGA-CMC had almost completely degraded during implantation time (Δ 86.9%) with only 13.1% remaining at 12 weeks. In contrast, BioOss granules showed minimal degradation (Δ 12.2%), with still 19.7% remaining at 12 weeks.

Bone formation. Histomorphometric results concerning material degradation are presented in Table 2. Overall, statistical testing revealed that bone formation increased significantly for both BioOss ($p<0.001$) and CPC-PLGA-CMC ($p<0.001$) during implantation time. Further, the statistical analysis indicated that no significant bone difference existed between bone formation at 4 and 12 weeks between BioOss and CPC-PLGA-CMC ($p>0.5$).

The results of the statistical analysis using an independent sample *T*-test for Equality of Means are presented in

Table 2. Histomorphometric Data of Bone Formation and Material into the Bone Defect

	Material	*4 weeks*	*12 weeks*	*Δ %*	p
Bone formation (%)	BioOss®	3.3 ± 6.4	47.6 ± 7.0	+44.3	<0.001
	CPC-PLGA-CMC	0 ± 0	44.8 ± 17.2	+44.8	<0.001
Amount of material (%)	BioOss	31.9 ± 9.3	19.7 ± 7.9	−12.2	<0.05
	CPC-PLGA-CMC	100 ± 0	13.1 ± 11.7***	−86.9	<0.001

$n=8$ for all specimens and implantation times.
***$p<0.001$ compared to BioOss.

Table 2. Further, the amount of material as left in the bone defects decreased significantly for both BioOss and CPC-PLGA-CMC from 4 to 12 weeks of implantation, showing that the highest decrease for CPC-PLGA-CMC was more enhanced.

Discussion

There is a clear need for synthetic bone graft materials that have appropriate handling properties and are able to support the predictable regeneration of bone defects. The benefit of using a grafting material based on the use of CPC is obvious, as cement-like materials are injectable, can be molded into shape and have a perfect fit with the bone defect borders. In addition, CPCs show excellent biological performance by supporting bone formation and apposition.[35] In the current study, a recently developed CPC-PLGA-CMC material was used for the regeneration of a critical-sized mandibular bone defect in a minipig experimental animal model. For comparative reasons, the study included also bone defects filled according to the predicate approach utilizing BioOss granules covered with a degradable GBR membrane. Histology and histomorphometry showed that both CPC-PLGA-CMC and BioOss induced similar amounts of bone formation into the bone defect after 12 weeks of implantation.

However, the degradation rate of CPC-PLGA-CMC was enhanced compared to the BioOss granules, as the CPC-PLGA-CMC had almost completely degraded during implantation time, while the BioOss showed minimal degradation (Δ 12.2%), with still 19.7% remaining at 12 weeks. This is in line with previously described *in vivo* data of small animal studies[21,33,36] For example, Grosfeld et al demonstrated that in a rabbit femoral bone defect model, BioOss particle degradation was marginal after 6 weeks of implantation in contrast to CPC-PLGA-CMC. The study also showed a continuous temporal increase in bone formation for CPC-PLGA-CMC after 26 weeks of healing.[21]

BioOss particle, which is a bovine inorganic bone graft substitute, is a commonly used biomaterial for the reconstruction of maxillofacial bone.[37,38] The current study confirmed that BioOss in combination with a GBR membrane favors the healing of a critical-sized mandibular bone defect. However, it has to be noticed that the bone regenerative capacity of BioOss varies between the published reports.[33,39,40] For example, Klijn et al performed a meta-analysis of total bone volume (TBV) and healing time of various bone graft materials used for sinus floor augmentation.[39] TBV is a significant parameter of the functioning of a bone graft material. They observed that TBV ranged from 8% to 47% after a healing time of 4–7 months. This variance in biological performance can be due to differences in composition between various batches of BioOss in combination with the amount (volume) of BioOss particles as applied into a bone defect.

Mladenovic et al observed in an *in vitro* study that the concentration of the element Si, as released in cell culture medium, shows variation between samples.[41] Si is known to be an important mineral for bone formation and an increased Si intake accelerates bone mineralization as well as increases bone mineral density.[40] Importantly, this effect of differences in Si concentration between BioOss batches can be further enhanced by the number of particles as placed into the bone defect.

Histomorphologic assessment of the biodegradability of the BioOss particles demonstrated that the grafted defects showed a decreasing pattern of remaining particle area fraction during implantation time. This is not surprising, because BioOss is known to degrade slowly and can persist for years after implantation.[42] The main component of BioOss is bone mineral, that is, a modified form of HA, which is considered to be one of the most stable CaP phases.[43] Consequently, the biodegradation of BioOss takes predominant place via phagocytosis by monocytes/macrophages or acidic mechanisms via osteoclasts as available in the bone remodeling process, which will be a slow process.[44] The cellular degradation can be affected by the BioOss particle size, but will in general proceed slowly due to the low number of macrophages and osteoclasts present after the initial bone healing response and depend on the bone remodeling activity.[45]

In contrast, examination of the CPC-PLGA-CMC specimens showed a reduction of 90% of the material between 4 and 12 weeks of implantation. This degradation behavior of the CPC-PLGA-CMC is largely due to the degradation of the PLGA particles, which is complete within about 8 weeks after implantation.[46] PLGA particles degrade hydrolytically into lactic and glycolic acids, creating a mild local acidity in the cement, which dissolves the CPC and results in an increase of the exposed cement surface.[27,47] As confirmed in the histological sections, the created space by cement resorption was occupied by the ingrowth of bone.

Considering bone formation, it is reasonable to assume that the released Ca and P due to cement dissolution had a beneficial effect on bone regeneration in the CPC-PLGA-CMC-grafted bone defects. Both Ca and P ions play a major role in the development and mineralization of bone.[48,49] For example, calcium promotes the recruitment of mesenchymal stem cells (MSCs) into a bone defect and has over time a paracrine effect on the expression of numerous endogenous cytokines relevant for MSC differentiation add proliferation.[50] Inorganic phosphorus has been reported to be essential for osteocyte differentiation as well as extracellular matrix mineralization and maturation of osteoblasts into osteocytes.[51]

In view of the above mentioned, it has also to be noticed that the BioOss- and CPC-PLGA-CMC-grafted defects showed a different pattern of bone regeneration. The BioOss particles formed a porous complex supporting the ingrowth and guidance of bone from the surrounding wall of the bone defect. In addition, new bone formation was limited to the particles as present within the defect area and did not extend between the BioOss particles, which were pushed during surgery into the bone marrow cavity. After 12 weeks of implantation, the regenerated bone had a cancellous appearance. In contrast, bone healing in the CPC-PLGA-CMC-filled defects seemed to be initiated at the periosteal side as well as the bone defect walls. In particular at the periosteal side, the cement was observed to be degraded completely and the resulting space became at the same rate filled with newly formed bone.

However, bone formation in the CPC-PLGA-CMC specimens occurred also in the cement that penetrated into

the bone marrow. Here, cement degradation and bone ingrowth proceeded at a slower pace and bone was now present in between cement remnants. We suppose that bone formation in this area is also due to dissolution of Ca and P resulting in a high bioactivity of the cement. Further, it was observed that the density of the bone structure at the periosteal side was higher compared with the bone marrow side, but still distinct from natural cortical bone. An explanation for the enhanced degradation of CPC-PLGA-CMC can be the difference in inflammatory response between the periosteal and endosteal side of the bone defect.

A severe trauma is induced at the buccal mandibular side due to the incision through skin, muscle layers, as well as the periosteal elevation, while the trauma in the bone marrow is very limited due to the careful bone preparation procedure and avoiding deep penetration of the trephine drill into the bone marrow (i.e., bleeding of the bone marrow during surgery was absent or very minimal).[52] Restriction of the inflammatory response due to the surgical trauma will be enhanced for the cement-filled defects, as the cement acts like the cork in a bottle and separates the buccal mandibular side completely from the endosteal side. As a consequence, the increased concentration of inflammatory cells will stay localized at the buccal mandibular side and cannot penetrate deeper into the bone defect. The intensified inflammatory reaction and the involved inflammatory cells will have a strong effect on CPC-PLGA-CMC degradation.

One of the most important aspects in GBR is the preservation of the three-dimensional architecture of a bone defect. Clinically, resorbable membranes in combination with BioOss® bone particles represent the state-of-the-art in current GBR procedures. The advantage of these resorbable membranes is that they degrade in time without the need for a second surgical procedure to remove the membrane. The downside of these membranes, however, is their limited mechanical strength and fast degradation that can cause a collapse of the bone defect. This has a negative influence on bone formation, especially in a large bone defect.[53] In contrast, the application of a CPC-PLGA-CMC cement could prevent this problem. Our data indicated that after 4 weeks, the material was dimensionally stable and stayed long enough within the bone defect to maintain space for bone regeneration.

An important aim of the current study was to prove that CPC-PLGA-CMC would be suitable as a moldable bone substitute with appropriate handling properties for craniomaxillofacial bone regenerative treatment without the need for the use of an additional GBR membrane. Our data indicated that CPC-PLGA-CMC has indeed appropriate handling properties, fills the bone defect completely, and has an appropriate setting time that fits within an acceptable clinical window.

Further, the cement stayed long enough within the bone defect to maintain space for bone regeneration without the need of using additional membrane coverage, and enabled transfer of mechanical stability from material to newly formed bone. Likely, the clinical handling properties of the cement can be further improved by delivering it as an injectable material, as this will further simplify and standardize the mixing of the powder and liquid into a paste as well as the application of the cement into a bone defect.

Conclusion

This minipig study showed that CPC-PLGA-CMC can easily be applied as a bone-grafting material, filling up the entire bone defect. Biologically, CPC-PLGA-CMC stimulates bone regeneration to a comparable extent as BioOss particles. Since CPC-PLGA-CMC degrades much faster compared to BioOss, is easier to apply into a bone defect, and does not need the use of an additional GBR membrane, our data support further investigation of CPC-PLGA-CMC toward human clinical trials.

Acknowledgments

The authors thank Natasja van Dijk and Vincent Cuijpers for preparing the histological MMA sections and histomorphometric analysis.

Authors' Contributions

All persons listed as authors declare that they have participated significantly in the work, including participation in the concept, design, analysis, writing, or revision of the article.

Disclosure Statement

Opinions, interpretations, conclusions, and recommendations are those of the author(s) and are not necessarily endorsed by the Department of Defense.

Funding Information

This work was supported by the Army, Navy, NIH, Air Force, VA and Health Affairs to support the AFIRM II effort, under award no. W81XWH-14-2-0004. The U.S. Army Medical Research Acquisition Activity, 820 Chandler Street, Fort Detrick, MD 21702–5014 is the awarding and administering acquisition office.

References

1. The Insight Partners. Dental Implants Market to 2027—Global Analysis and Forecasts by Product (Dental Bridges, Dental Crowns, Dentures, Abutments, and Others); Material (Titanium Implants & Zirconium Implants); End User (Hospitals & Clinics, Dental Laboratories, and Others) and Geography; 2019. Available from: http://theinsightpartners.com [Last accessed: November 6, 2019].
2. Bornstein MM, Halbritter S, Harnisch H, et al. A retrospective analysis of patients referred for implant placement to a specialty clinic: Indications, surgical procedures, and early failures. Int J Oral Maxillofac Implants 2008;23:1109–1116.
3. Chiapasco M, Zaniboni M, Boisco M. Augmentation procedures for the rehabilitation of deficient edentulous ridges with oral implants. Clin Oral Implants Res 2006;17(Suppl. 2):136–159.
4. Lindhe J, Lindhe J, Lang NP, et al. Clinical Periodontology and Implant Dentistry, 6th ed. Wiley: Hoboken, NJ, USA; 2015.
5. Pietrokovski J, Massler M. Alveolar ridge resorption following tooth extraction. J Prosthet Dent 1967;17(1):21–27.
6. Tan WL, Wong TL, Wong MC, et al. A systematic review of post-extractional alveolar hard and soft tissue dimensional changes in humans. Clin Oral Implants Res 2012:23 (Suppl.):1–21.

7. Schropp L, Wenzel A, Kostopoulos L, et al. Bone healing and soft tissue contour changes following single-tooth extraction: A clinical and radiographic 12-month prospective study. Int J Periodontics Restorative Dent 2003;23(4):313–323.
8. Elgali I, Omar O, Dahlin C, et al. Guided bone regeneration: Materials and biological mechanisms revisited. Eur J Oral Sci 2017;125(5):315–337.
9. Khojasteh A, Kheiri L, Motamedian SR, et al. Guided bone regeneration for the reconstruction of alveolar bone defects. Ann Maxillofac Surg 2017;7(2):263–277.
10. Liu J, Kerns DG. Mechanisms of guided bone regeneration: A review. Open Dent J 2014;8:56–65.
11. Cucchi A, Chierico A, Fontana F, et al. Statements and recommendations for guided bone regeneration: Consensus report of the guided bone regeneration symposium held in Bologna, October 15 to 16, 2016. Implant Dent 2019;28(4): 388–399.
12. Lee SW, Kim SG. Membranes for the guided bone regeneration. Maxillofac Plast Reconstr Surg 2014;36(6):239–246.
13. Rasia-dal Polo M, Poli PP, Rancitelli D, et al. Alveolar ridge reconstruction with titanium meshes: A systematic review of the literature. Med Oral Patol Oral Cir Bucal 2014;19(6):e639–e646.
14. Soldatos NK, Stylianou P, Koidou VP, et al. Limitations and options using resorbable versus nonresorbable membranes for successful guided bone regeneration. Quintessence Int 2017;48(2):131–147.
15. Benic GI, Hämmerle CHF. Horizontal bone augmentation by means of guided bone regeneration. Periodontology 2000 2014;66(1):13–40.
16. Veríssimo DM, Leitão RF, Figueiró SD, et al. Guided bone regeneration produced by new mineralized and reticulated collagen membranes in critical-sized rat calvarial defects. Exp Biol Med (Maywood) 2015;240(2):175–184.
17. Wang HL, Boyapati L. ''PASS'' principles for predictable bone regeneration. Implant Dent 2006;15(1):8–17.
18. Greenstein G, Cavallaro B, Elian J, et al. Flap advancement: Practical techniques to attain tension-free primary closure. J Periodontol 2009;80:4–15.
19. Brown WE. A new calcium phosphate, water-setting cement. Cem Res Progr 1987:351–379.
20. LeGeros RZ. Calcium phosphate materials in restorative dentistry: A review. Adv Dent Res 1988;2(1):164–180.
21. Grosfeld EC, Hoekstra JWM, Herber RP, et al. Long-term biological performance of injectable and degradable calcium phosphate cement. Biomed Mater 2016;12(1):015009.
22. Bohner M. Calcium orthophosphates in medicine: From ceramics to calcium phosphate cements. Injury 2000;31(Suppl. 4): 37–47.
23. Apelt D, Theiss F, El-Warrak AO, et al. In vivo behavior of three different injectable hydraulic calcium phosphate cements. Biomaterials 2004;25(7–8):1439–1451.
24. Dorozhkin SV. Calcium orthophosphate cements for biomedical application. J Mater Sci 2008;43(9):3028–3057.
25. Bohner M. Design of ceramic-based cements and putties for bone graft substitution. Eur Cell Mater 2010;20:1–12.
26. Yamada S, Heymann D, Bouler JM, et al. Osteoclastic resorption of calcium phosphate ceramics with different hydroxyapatite beta-tricalcium phosphate ratios. Biomaterials 1997;18(15):1037–1041.
27. Liao H, Walboomers XF, Habraken WJ, et al. Injectable calcium phosphate cement with PLGA, gelatin and PTMC microspheres in a rabbit femoral defect. Acta Biomater 2011;7(4):1752–1759.
28. Lodoso-Torrecilla I, van den Beucken JJJP, Jansen JA. Calcium phosphate cements: Optimization toward biodegradability. Acta Biomater 2021;119:1–12.
29. van Oirschot B, Jansen JA, van de Ven C, et al. Evaluation of collagen membranes coated with testosterone and alendronate to improve guided bone regeneration in mandibular bone defects in minipigs. J Oral Maxillofac Res 2020;11(3):e4.
30. FDA report K131385. Contract No.: FDA report K131385. Easy-graft, bone grafting materials, synthetic. Degradable Solutions AG.
31. FDA Report K033815. Contract No.: FDA Report K033815. Bio-oss-Bio-oss Blocks, Bio-oss Collagen, Geistlich Pharma AG.
32. Jensen SS, Yeo A, Dard M, et al. Evaluation of a novel biphasic calcium phosphate in standardized bone defects: A histologic and histomorphometric study in the mandibles of minipigs. Clin Oral Implants Res 2007;18(6):752–760.
33. Dau M, Kammerer PW, Henkel KO, et al. Bone formation in mono cortical mandibular critical size defects after augmentation with two synthetic nanostructured and one xenogenous hydroxyapatite bone substitute—In vivo animal study. Clin Oral Implants Res 2016;27(5):597–603.
34. van Oirschot B, Geven EJW, Mikos AG, et al. A mini-pig mandibular defect model for evaluation of craniomaxillofacial bone regeneration. Tissue Eng Part C Methods 2022;28(5):193–201.
35. Klijn RJ, van den Beucken JJ, Felix Lanao RP, et al. Three different strategies to obtain porous calcium phosphate cements: Comparison of performance in a rat skull bone augmentation model. Tissue Eng Part A 2012;18(11–12):1171–1182.
36. He H, Qiao Z, Liu C. Accelerating biodegradation of calcium phosphate cement. In: Developments and Applications of Calcium Phosphate Bone Cements. Springer Series in Biomaterials Science and Engineering, Vol. 9. (Liu C, He H. eds.); Springer: Singapore; 2018.
37. Akbarzadeh Baghban A, Dehghani A, Ghanavati F, et al. Comparing alveolar bone regeneration using Bio-Oss and autogenous bone grafts in humans: A systematic review and meta-analysis. Iran Endod J 2009;4(4):125–130.
38. de Carvalho Moreira A, Silva JR, de Paula Samico R, et al. Application of Bio-Oss in tissue regenerative treatment prior to implant installation: Literature review. Braz Dent Sci 2019;22(2):147–154.
39. Klijn RJ, Meijer GJ, Bronkhorst EM, et al. A meta-analysis of histomorphometric results and graft healing time of various biomaterials compared to autologous bone used as sinus floor augmentation material in humans. Tissue Eng Part B-Re 2010;16(5):493–507.
40. Price CT, Koval KJ, Langford JR. Silicon: A review of its potential role in the prevention and treatment of postmenopausal osteoporosis. Int J Endocrinol 2013;2013.
41. Mladenovic Z, Sahlin-Platt A, Andersson B, et al. In vitro study of the biological interface of Bio-Oss: Implications of the experimental setup. Clin Oral Implants Res 2013;24(3): 329–335.
42. Artzi Z, Givol N, Rohrer MD, et al. Qualitative and quantitative expression of bovine bone mineral in experimental bone defects. Part 2: Morphometric analysis. J Periodontol 2003;74(8):1153–1160.
43. Lu JX, Gallur A, Flautre B, et al. Comparative study of tissue reactions to calcium phosphate ceramics among cancellous, cortical, and medullar bone sites in rabbits. J Biomed Mater Res 1998;42(3):357–367.

44. Sheikh Z, Abdallah M-N, Hanafi AA, et al. Mechanisms of in vivo degradation and resorption of calcium phosphate based biomaterials. Materials 2015;8(11):7913–7925.
45. Lu J, Descamps M, Dejou J, et al. The biodegradation mechanism of calcium phosphate biomaterials in bone. J Biomed Mater Res 2002;63(4):408–412.
46. Habraken WJ, Wolke JG, Mikos AG, et al. Injectable PLGA microsphere/calcium phosphate cements: Physical properties and degradation characteristics. J Biomater Sci Polym Ed 2006;17(9):1057–1074.
47. An J, Liao H, Kucko NW, et al. Long-term evaluation of the degradation behavior of three apatite-forming calcium phosphate cements. J Biomed Mater Res A 2016;104(5): 1072–1081.
48. Sethi A, Priyadarshi M, Agarwal R. Mineral and bone physiology in the foetus, preterm and full-term neonates. Semin Fetal Neonatal Med 2020;25(1):101076.
49. Roschger A, Wagermaier W, Gamsjaeger S, et al. Newly formed and remodeled human bone exhibits differences in the mineralization process. Acta Biomater 2020;104:221–230.
50. Aquino-Martinez R, Monroe DG, Ventura F. Calcium mimics the chemotactic effect of conditioned media and is an effective inducer of bone regeneration. PLoS One 2019;14(1):e0210301.
51. Zhang R, Lu Y, Ye L, et al. Unique roles of phosphorus in endochondral bone formation and osteocyte maturation. J Bone Miner Res 2011;26(5):1047–1056.
52. Lord JM, Midwinter MJ, Chen YF, et al. The systemic immune response to trauma: An overview of pathophysiology and treatment. Lancet 2014;384(9952): 1455–1465.
53. Pihlstrom BL, Michalowicz BS, Johnson NW. Periodontal diseases. Lancet 2005;366(9499):1809–1820.

Address correspondence to:
Bart van Oirschot, DDS, PhD
Department of Dentistry—Regenerative Biomaterials
Radboud University Medical Center
Philips van Leijdenlaan 25
Nijmegen 6525 EX
The Netherlands

E-mail: bart.vanoirschot@radboudumc.nl

Received: October 4, 2022
Accepted: November 28, 2022
Online Publication Date: January 30, 2023